EXPERIMENTAL AND NUMERICAL STUDY OF A NEAR-FIELD POLLUTANTS DISPERSION CAMPAIGN IN A STRATIFIED SURFACE LAYER

Xiao Wei[1], Eric Dupont[1], Bertrand Carissimo[1], Eric Gilbert[1] and Luc Musson-Genon[1]

[1]Research and Teaching Centre in Atmospheric Environment (CEREA), EDF R&D, Chatou, France

Abstract: In order to study pollutants dispersion in a stably stratified surface layer at small scales, a field experiment program is being conducted on the site 'SIRTA' in the southern suburb of Paris. Data analysis is made on turbulence and concentration measurements during an IOP (Intensive Observation Period). Turbulence is characterized to be strongly anisotropic in a stable surface layer. Forest to the north of experiment field induces a strong wind directional shear between 3 m and 30 m levels and a wind speed decrease. Concentration measurements are influenced by plume meandering effect which occurs usually in a stable condition. Numerical simulation in RANS mode with a canopy model enables to reproduce qualitatively the observed wind rotation and the shelters effect on turbulence kinetic energy, but there is still difference in values between measurements and simulation results which can be partly explained by the uncertainty on the inlet profiles.

Key words: atmospheric dispersion, coherent structure, Code_Saturne, stable atmosphere, turbulence

INTRODUCTION

Pollutants dispersion in a stable atmospheric boundary layer and in complex environment is still a phenomenon that is relatively poorly described by modelling and difficult to reproduce in a wind tunnel. Nevertheless, this topic is of major interest in the field of air pollution from human activities such as industrial risks and road transportation, as stable conditions induce large fluctuations of pollutants concentrations with possible occurrence of very high values. An experimental program consisting in measuring pollutants dispersion in a stratified surface layer and in near-field (less than 200m) is carried out on the site SIRTA (Instrumental Site Research by Atmospheric Remote Sensing), on the campus of the Ecole Polytechnique, about 20 km south of Paris. The aim of this experimental program is to characterize the fine structure of turbulence and associated dispersion through high temporal and spatial resolution collocated measurements in a real site, and to find expected relationships between concentration fluctuation and passage of turbulence structure particularly in a stable atmospheric boundary layer.
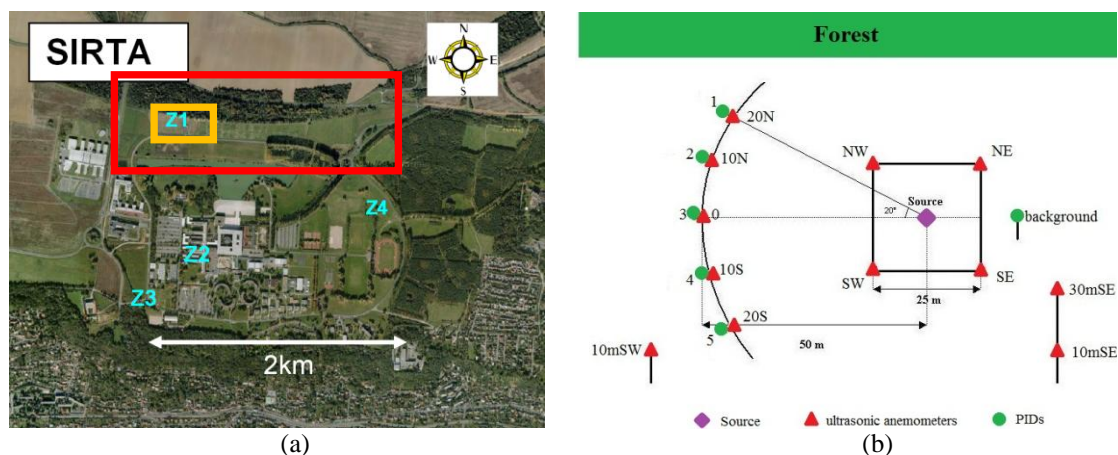

(a)
(b)

Figure 1. (a) Whole measurement area in the SIRTA field (red rectangular: modelling area; yellow rectangular: instrumented area) and (b) sensors positions in Zone 1

Figure 1(a) shows the different measurement areas of the SIRTA site. Our campaign is carried out in Zone 1, which is limited in the north by a forest and in the south by a road (which is close to traffic during the release experiments). Figure 1(b) shows position of sensors used for this experiment. We have 12 ultrasonic anemometers measuring wind velocity (u, v, w) (in meteorological reference) and sound velocity (from which is derived the "sonic" air temperature T) at 10 Hz, and 6 photo-ionization detectors (PIDs) measuring tracer gas (propylene) concentration at 50 Hz. Turbulence measurements have been recorded continuously for more than two years (since April 2012), while concentration measurements have been performed only during short (about 1 hour) gas releases for specific meteorological conditions (tracer tests). Main characteristics of the program, the site, required meteorological conditions during tracer tests, devices information and sensors positions have been all described in details in Wei et al. (2014). In the following, all the sensors will be identified with the same names as in Figure 1(b).

Intensive observation periods (IOPs) with gas releases have been performed since March 2012, an IOP on 5th June 2013 (from 18:48 to 20:17) has been chosen to present the results because of better quality PIDs measurements. This paper first introduces briefly turbulence characteristics in this IOP. Then, it presents data processing and analysis for concentration measurements. Finally, it illustrates methods and first results in numerical simulations.

SONIC DATA ANALYSIS
Same procedures of sonic data processing and analysis have been applied as presented in Wei et al. (2014). Variables such as mean wind direction dd_{mean} and velocity a_{mean}, variances of the 3 wind components $(\sigma_a^2, \sigma_b^2, \sigma_w^2)$, turbulent kinetic energy TKE, friction velocity u_*, vertical heat flux Q_0 and Monin-Obukhov length L_{MO}, are reported in table 1, in which a and b are streamwise and crosswind components of the velocity, and dd is the horizontal wind direction. They have been calculated over a sub-period of about 60 min in the IOP (from 19:08 to 20:08) during which meteorological conditions are almost stationary. Integral length scales L for three velocity components have also been deduced from velocity autocorrelation. The turbulence characteristics are similar to those found in IOP on 21 March 2013 (Wei et al., 2014). Turbulence strong anisotropy is quantified by different order of magnitude between variances $(\sigma_a^2, \sigma_b^2, \sigma_w^2)$ and integral length scales (L_{aa}, L_{bb}, L_{ww}) in our stable surface layer. Wind direction and velocity have always a lag between measurements from anemometers on the north and on the south due to the perturbation from the forest to the north of Zone 1. The turbulent structures advection speed obtained by velocity cross-correlation between sensors at 3 m above ground level is higher than the measured average wind speed at this height, as previously reported in Horst et al. (2004). Velocity spectra show several slopes in different frequency regions. In addition to -5/3 slope representing the inertial subrange, a -1 slope has been found at intermediate frequency region in all the spectra, including the vertical component's one especially at height of 3 m, which was not the case in Drobinski et al. (2004) for near-neutral situations.

Table 1. Statistical values of 12 anemometers calculated from the 60 min sub-period data of the IOP on 5th June 2013

	NE	NW	SE	SW	20N	10N	0	10S	20S	10mSW	10mSE	30mSE
height (m)	3	3	3	3	3	3	3	3	3	10	10	30
dd_{mean} (°)	111.5	106.8	95.0	96.1	108.0	94.1	94.9	90.2	92.4	75.4	71.7	58.2
a_{mean} (ms^{-1})	0.92	1.00	1.63	1.83	1.22	1.39	1.43	1.59	1.68	2.06	2.42	3.54
σ_a^2 (m²s^{-2})	0.44	0.53	0.54	0.61	0.48	0.50	0.61	0.51	0.56	0.67	0.81	1.29
σ_b^2 (m²s^{-2})	0.30	0.33	0.50	0.49	0.38	0.40	0.42	0.48	0.48	0.52	0.52	0.77
σ_w^2 (m²s^{-2})	0.10	0.12	0.13	0.13	0.11	0.13	0.14	0.14	0.14	0.25	0.25	0.32
TKE (m²s^{-2})	0.42	0.49	0.59	0.61	0.49	0.51	0.59	0.56	0.59	0.72	0.79	1.19
u_* (ms^{-1})	0.21	0.23	0.26	0.25	0.22	0.23	0.24	0.25	0.28	0.36	0.37	0.53
Q_0 (Kms^{-1})	-0.03	-0.06	-0.03	-0.06	-0.03	-0.03	-0.04	-0.04	-0.05	-0.02	-0.03	-0.03
L_{MO} (m)	21	16	40	20	24	26	24	31	34	176	131	416
L_{aa} (m)	14.82	13.13	14.86	16.69	19.62	19.67	19.50	13.99	14.28	33.31	-	91.95
L_{bb} (m)	5.67	6.42	11.11	12.47	7.68	9.56	8.46	10.81	12.27	11.51	16.00	24.76
L_{ww} (m)	1.83	2.00	1.96	2.02	2.07	2.08	2.15	2.07	2.35	5.96	7.27	8.84

CONCENTRATION DATA ANALYSIS
During the IOP on 5th June the PIDs measured correctly except PID 4 which could not detect gas concentration. Raw data obtained from PIDs is gas concentration in ppm (parts-per-million, 10^{-6}) at 50

Hz. First, negative values as invalid data are eliminated by linear interpolation of its neighbours that have non-negative values. Next, inspired by Mylne (1992), a similar baseline method has been applied to remove sensor drift and background concentration from each PID measurement. The baseline is deducted from the average of the 200 smallest values every 5min. We obtain the concentration data ready for statistical analysis plotted in figure 2. We observe that PIDs 1, 2, and 3 detected most of the concentration peaks, which is consistent with the wind direction during the IOP which is slightly South-East. We draw also concentration histograms for the release period (not shown). Log-normal distributions were obtained for all the PIDs' data except that the PID background's histogram is much narrower than others. These histograms forms indicate that 50 m from the source is still a near-source region where we might be influenced by plume meandering effect because PIDs at 50 m detected very high concentration values but in small number.
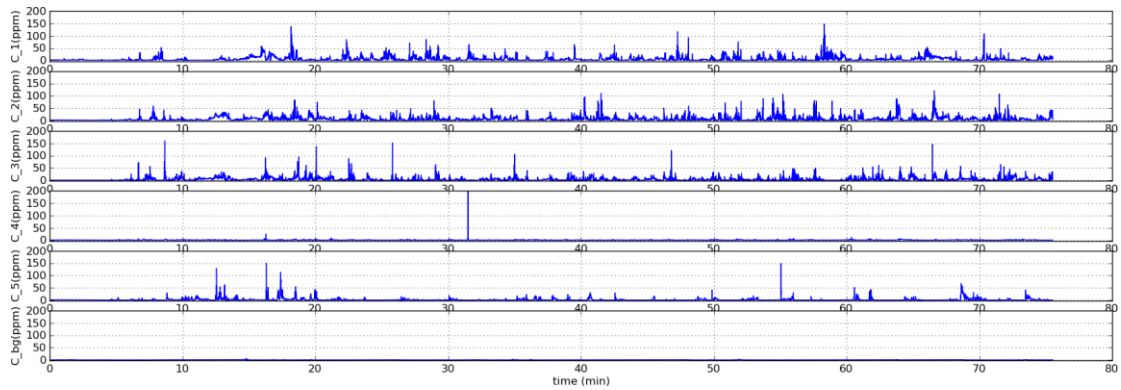

Figure 2. Concentration data after value correction for the IOP on 5th June 2013 (from 18:48 to 20:17) for PIDs (from top to bottom) 1, 2, 3, 4, 5 and background

Table 2. Statistical values of PIDs during IOP on 5th June 2013

	PID 1	PID 2	PID 3	PID 5	PID background
Height (m)	3	3	3	3	3
I	0.52	0.54	0.41	0.18	0.00
C (ppm)	5.46	5.58	3.87	1.79	0.25
C_P (ppm)	9.72	9.62	8.68	7.83	-
σ_c (ppm)	7.98	8.19	7.10	5.07	0.25
σ_c/C	1.46	1.47	1.83	2.84	0.98
$(\sigma_c/C)_P$	0.82	0.85	0.82	0.65	-
L_C (m)	6.29	6.52	3.12	12.91	-

Statistical values such as intermittency factor I (probability that the concentration is non-zero), mean concentration C, conditional mean C_P, standard deviation of concentration σ_c, fluctuation intensity σ_c/C, conditional intensity $(\sigma_c/C)_P$ are presented in table 2, where the subscript P is used to indicate that the statistical parameter is calculated from non-zero concentration only. In our case, a threshold value $C_T=2$ ppm has been chosen to define the non-zero concentration in order to ensure that real tracer gas concentration can be distinguished from background and instrumental noise. So those conditional statistical parameters are obtained based on concentrations larger than the threshold value C_T. Intermittency factors and mean concentrations have higher values for PID located in the north especially for PID 1 and 2 which is coherent with the south-easterly wind measured at 3 m height. Great differences are found between non-conditional and conditional statistical parameters (C and C_P, σ_c/C and $(\sigma_c/C)_P$), and conditional statistical values are almost constants between all the PIDs. Also, we deduce integral length scales of plume L_C from concentration auto-correlation and find that they are in good agreement with the transversal wind component's integral length scale L_{bb} of the collocated anemometers. The statistical analyses show that, at 50 m from the source in a stable condition like ours, turbulence eddies seems to have larger scales than the plume and they cause the plume to meander. As pointed out in Mylne (1992), measurements made under stable condition are strongly influenced by the effect of plume meandering which is believed to be caused by large two-dimensional eddies. In our case, the plume

meandering effect plays probably an important role in concentration measurements, and the crosswind velocity has more effect than other components on plume meandering.
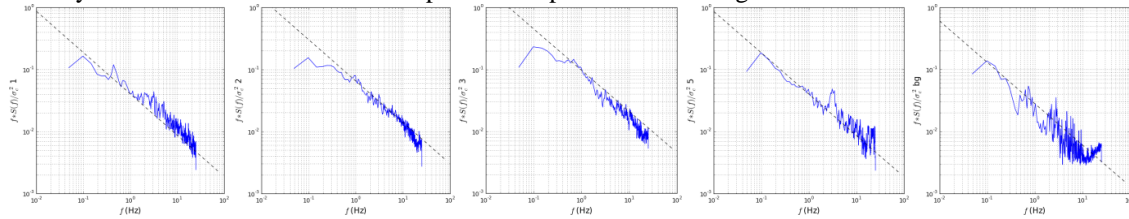

Figure 3. Normalized concentration spectra $fS(f)/\sigma_C^2$ for PIDs (from left to right) 1, 2, 3, 5 and background during IOP on 5th June 2013, dashed lines on the graph indicate -2/3 slope for comparison

Normalized concentration spectra $fS(f)/\sigma_C^2$ are calculated for PID 1, 2, 3, 5 and background and plotted in figure 3. Spectra generally follow well the -2/3 slope showing the existence of the inertial subrange. Spectra of PID 5 and background are much more fluctuating than that of PID 1, 2 and 3, as they are on the edge of the plume and have an intermittency factor much smaller than others. Because of the intermittency effect, it is much more difficult to observe a clear inertial subrange in the measured concentration spectra (Mylne, 1992). However, we find that the spectrum of PID background shows somehow an inertial subrange, which implies that there might be other source around during the IOP.

NUMERICAL SIMULATION

Numerical simulations are performed by using an open source CDF code Code_Saturne co-developed by CEREA and Electricity de France (EDF). An area of dimension 1200 m × 500 m × 200 m in Zone 1 has been chosen for modelling (see modelling area in figure 1) with a progressive three-dimensional grid refined in the instrumented area and near the ground. The horizontal resolution ranges from 1 m in the instrumented area (180 m × 100 m, see figure 1) to 5 m for the rest of modelling area. The vertical grid resolution varies from 0.5 m near the ground until 10 m at height of 200 m. Shelters in the instrumented area have been taken into account explicitly in the mesh. The boundary conditions are defined as follows:

- Inlet condition: Dirichlet type with analytical profiles. In this paper, we used an analytical profile (VDI, 2002) generated with measurements of anemometers 10mSE and 30mSE in IOP on 5th June 2013 to run the simulation. The reference height is 30 m, and we have wind direction = 58°, wind velocity=3.5 ms⁻¹ and L_{MO}=131 m.
- Outlet condition: free outflow.
- The ground and shelters surfaces: a constant roughness equals to 0.1 m.

Concerning the modelling of forest area, a drag porosity model presented in Zaïdi et al. (2013) has been applied. A land-use cover file provided by the French Institute of Geography and manually corrected on the basis of satellite photographs has been used to identify the different land cover types (forest, low vegetation area, water, etc.) and give them a correspondent roughness length z_0. Then, for the forest area, we applied the drag porosity model by adding a source term in the Navier-Stockes momentum equation and two other terms in the k and ε equations. These terms create an aerodynamic drag against the flow, cause decrease in wind speed and modify turbulence.

Simulations are first made in RANS mode with standard k-ε turbulence model and stable thermal stratification taken into consideration. The goal is to check that Code_Saturne is able to reproduce correctly the mean flow on the experiment area. Results such as velocity and TKE fields are shown in figure 4. They are consistent with the phenomena found in measurements. Figure 4(a) shows the wind channelling effect of the forest on the velocity. We can see more clearly in figure 4(b) that the forest to the north of the instrumented area slows down the wind and changes its direction, which can explain why the mean wind direction measured by anemometers in the north is always more south-east than that measured by those in the south, and the mean wind velocity measured in the north is always smaller than that measured in the south (see table 1). From figure 4(c), we observe that TKE has lower values close to the forest, and has higher values behind shelters. This is the reason for relatively high TKE values given by anemometers SE, SW and 20S in table 1. Moreover, we find that pressure field (not shown) of

simulations shows a slightly smaller pressure in forest area. Besides the forest wind channelling effect, this pressure difference, which is of order of few Pascal, is another contribution to the wind rotation.
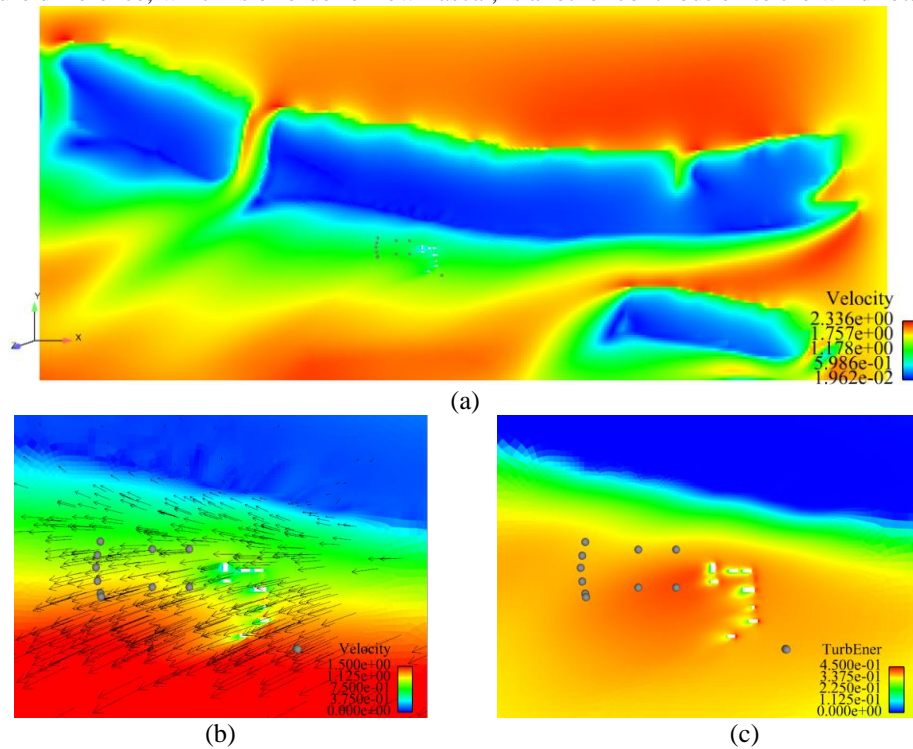

Figure 4. Simulation results at 3m level of (a) velocity field for Zone 1, (b) velocity field with wind vector for instrumented area, and (c) TKE field for instrumented area

Comparison between measurements and simulations has also been made for this case. Regardless of the coherent variation trend between simulation profiles and measurements in wind direction and velocity and turbulent kinetic energy, there is still difference in values. Wind velocity obtained from simulation is about 20% smaller than the measurements, especially for anemometers in the south. Simulated wind velocity is much more north-east than measurements at 3 m height because simulation can't reproduce exactly the wind deviation effect of the forest. TKE in simulation is much smaller than measurements especially at height of 30 m. These differences between calculated and measured values might be due at least partly to the inlet profiles which are not measured and therefore have to be built with theoretical profiles and measurements inside the simulation domain. These measurements contain already a perturbation from the environment and might be different from the real situation at the inlet of the domain.

CONCLUSION AND FUTURE WORKS
In this paper, we introduced data analysis results for turbulence and concentration during an IOP and preliminary results for simulations of pollutants dispersion. Turbulence strong anisotropy has been quantified in our stable surface layer. Perturbation from the forest to the north of zone 1 seems to slow down wind velocity and change wind direction. Concentration measurements showed the evidence of plume meandering effect in stable stratified surface layer. It seems that crosswind velocity has more effect than other components on plume meandering, since we found coherent values between integral length scales of crosswind velocity L_{bb} and that of the plume L_C. Inertial subrange has been also identified in the concentration spectra, even in the spectrum of PID background which implies that there might be other propylene source around during the IOP. Simulations have been run for zone 1 domain with a canopy model and standard k-ε method in stable condition. Simulations can reproduce qualitatively wind channelling effect of forest on velocity and impact of shelters on turbulence kinetic energy. However, specific values are different between simulations and measurements due possibly to an inaccurate inlet profile.

In the future, we are going to analyse continuous turbulence data over two years, in order to see how turbulence characteristics vary with stability conditions. More PIDs are arriving which allows to extend the concentration measurements network. We will try to identify relationships between fluctuations of turbulence and concentration during IOPs. Numerical simulations will be continued in mode RANS with a second-order turbulence model R_{ij}-ε in order to model turbulence anisotropy. Concentration fluctuation model will be integrated in future simulations as well.

REFERENCES

Drobinski, P., P. Carlotti, R.K. Newsom, R.M. Banta, R.C. Foster, J. Redelsperger, 2004: The Structure of the Near-Neutral Atmospheric Surface Layer. *J. Atmos. Sci.*, **61**, 699–714.

Horst, T.W., J. Klessl, and D.H. Lenshow, 2004: HATS: Field Observations to Obtain Spatially Filtered Turbulence Fields from Crosswind Arrays of Sonic Anemometers in the Atmospheric Surface Layer. *Journal of the Atmospheric Sciences*, 61, 1566-1581.

Mylne, K.R., 1992: Concentration Fluctuation Measurements in a Plume Dispersing in a Stable Surface Layer. *Boundary Layer Meteorology*, **60**, 15–48.

VDI, 2002: Environmental meteorology Turbulence parameters for dispersion models supported by measurement data, Verein Deutscher Ingenieure, 3783-part 8.

Wei, X., E. Dupont, B. Carissimo, E. Gilbert, L. Musson-Genon, 2004 : A preliminary analysis of measurements from a near-field pollutants dispersion campaign in a stratified surface layer, *Int. J. Environ. Pollut.* in press.

Zaïdi, H., E. Dupont, M. Milliez., L. Musson-Genon and B. Carissimo, 2013: Numerical simulations of the microscale heterogeneities of turbulence observed on a complex site. *Boundary-Layer Meteor.,* 147, 237-259.